

Comparison of Methods for Acceptance and Constancy Testing in Dental Cone-beam Computed Tomography

Methodenvergleich zur Abnahme- und Konstanzprüfung in der dentalen digitalen Volumentomografie

Authors

C. Steiding, D. Kolditz, W. Kalender

Affiliation

Institute of Medical Physics, Friedrich-Alexander-University Erlangen-Nürnberg, Erlangen, Germany

Key words

- CT
- physics
- QA/QC
- technical aspects

received 30.6.2014
accepted 8.9.2014

Bibliography

DOI <http://dx.doi.org/10.1055/s-0034-1385333>
Published online: 12.11.2014
Fortschr Röntgenstr 2015; 187: 283–290 © Georg Thieme Verlag KG Stuttgart · New York · ISSN 1438-9029

Correspondence

Christian Steiding
Institute of Medical Physics,
Friedrich-Alexander-University
Erlangen-Nürnberg
Henkestr. 91
91052 Erlangen
Germany
Tel.: +49(91 31)8 52 55 34
Fax: +49(91 31)8 52 28 24
christian.steiding@imp.uni-erlangen.de

Zusammenfassung



Ziel: Das Ziel dieser Arbeit war die Anwendung, Validierung und der Vergleich zweier Konzepte zur Beurteilung der Bildqualität (BQ) in der dentalen digitalen Volumentomografie (DVT): 1. der 2013 neu eingeführte, deutsche Standard DIN 6868 – 161 und 2. der fest etablierte Standard IEC 61 223 – 3-5 von Röntgeneinrichtungen für klinische CT (nachfolgend als „DIN“ und „IEC“ bezeichnet).

Material und Methoden: Die approximierte, transversale Modulationsübertragungsfunktion (MÜF), der Homogenitätsindikator (H*) und Kontrast-Rausch-Indikator (KRI) wurden nach DIN bestimmt. Unter Hinzunahme eines kürzlich vorgestellten, IEC-entsprechenden Qualitätssicherungskonzeptes wurden Bildrauschen, der Homogenitätsindex (H), das Kontrast-Rausch-Verhältnis (KRV) und die 3D-MÜF mit einem modularen Prüfkörper gemessen. Alle Messungen wurden an einem klinischen DVT-Gerät durchgeführt. Beide Phantome wurden an variierenden z-Positionen platziert, um das Ausmaß der Bildartefakte zu untersuchen. Ein spezielles Computerprogramm wurde für die automatisierte Bildqualitätssicherung implementiert.

Ergebnisse: Die Detektion beider Prüfkörper erfolgte in den Messungen automatisiert und gewährleistete das reproduzierbare Platzieren der Auswerteregionen und -volumen. Die 50%- und 10%-MÜF-Werte nach approximierter und exakter Berechnungsmethode stimmten bis auf 5% überein. Mit zunehmendem axialen Abstand vom Messfeldzentrum fielen H* und KRI um 30% beziehungsweise 19%. Die konventionellen BQ-Parameter zeigten eine höhere Sensitivität gegenüber den Bildartefakten; H und KRV reduzierten sich um 197% und 37%.

Schlussfolgerung: Die automatisierten Qualitätssicherungsprozeduren offerieren eine zuverlässige

Abstract



Purpose: The aim of this work was to implement, validate, and compare two procedures for routine image quality (IQ) assurance in dental cone-beam computed tomography (CBCT): 1. the German standard DIN 6868 – 161 introduced in 2013 and 2. the established standard IEC 61 223 – 3-5 for clinical CT x-ray equipment referenced as “DIN” and “IEC” below.

Materials and Methods: The approximated in-plane modulation transfer function (MTF), the contrast-to-noise indicator (CNI), and the uniformity indicator (UI*) were determined in accordance with DIN. Image noise, the uniformity index (UI), the contrast-to-noise ratio (CNR), and the 3D MTF were measured according to IEC 61 223 – 3-5 using a previously proposed quality assurance (QA) framework. For this, a modular phantom was used. All experiments were performed on a clinical dental CBCT unit. The severity of image artefacts was measured at different z-positions. A dedicated computer program was implemented to allow for automated QA procedure.

Results: The position and orientation of the phantoms were detected automatically in all of the measurements providing a reproducible placement of the evaluation regions and volumes. 50% and 10% in-plane MTF values of the approximated and the exact MTF calculation procedure were in agreement to within 5%. With increasing axial distance from the isocentre, UI* and CNI dropped by 30% and 19%, respectively. Conventional IQ parameters showed higher sensitivity to image artefacts; i. e., UI and CNR were reduced by about 197% and 37%.

Conclusion: The implemented automated QA routines are compatible with both the DIN and the IEC approach and offer reliable and quantitative tracking of imaging performance in dental CBCT for clinical practice. However, there is no equivalent

ge und quantitative Beurteilung der Leistungsmerkmale zur Bildung in der DVT für die klinische Praxis. Es gibt keine Äquivalenz zwischen den BQ-Maßen nach DIN und IEC. Zudem wird die direkte Charakterisierung physikalischer Bildgebungseigenschaften in Form von Bildkontrast und -rauschen, Homogenität und axiale Ortsauflösung durch die neue DIN-Norm nicht unterstützt.

Kernaussagen:

- ▶ Gleichwertigkeit zwischen der neuen DIN 6868 – 161 und IEC 61 223 – 3-5 ist nicht gegeben.
- ▶ Rauschen, Homogenität und Kontrast sind gut zur Untersuchung von Bildartefakten geeignet.
- ▶ Das implementierte, automatisierte Qualitätssicherungsprogramm kann in der klinischen Routine eingesetzt werden.

Introduction

In the late 1990s, dedicated cone-beam computed tomography (CBCT) units were introduced for three-dimensional (3D) imaging of oral and maxillofacial structures [1, 2] and are widely used in clinical routine today [3–5]. As a basic principle, they consist of a device rotating circularly that is equipped with an x-ray source on one side and an image intensifier or a flat-panel detector on the opposite side [6] in order to acquire projection data for the volume data reconstruction process. These dental CBCT systems, sometimes labelled as digital volume tomography (DVT) scanners, feature high isotropic spatial resolution for a small field of view [7] at low dose [8] and with reasonable geometric accuracy [9]. In addition, dental CBCT implies relatively low investment in equipment and floor space requirement [2]. Consequently, this new technique has found increasing acceptance in dental and cranio-maxillofacial practice in the fields of image-guided treatment planning, orthodontics and traumatology [10–12].

As for all medical imaging devices, the overall system performance needs to be checked on a regular basis. However, to date there is still a lack of transnational consensus on acceptance and constancy testing for image quality (IQ) and dose of dental CBCT systems. Only national recommendations related to quality assurance (QA) and testing of equipment exist but are not generally consistent with one another (e.g. [13, 14]). This deficiency was recognized by the United States [15] and the European Union [16] with the result that “basic principles” on the use of dental CBCT were established. Even though a few previous studies [17–19] and special working groups (e.g. SEDENTEXCT project [20]) tried to formulate IQ testing procedures for dental CBCT, there is currently no consensus on the metrics needed to characterize volumetric dental CBCT system performance sufficiently in clinical practice. Previous work in the field of establishing QA standards differs in the amount, complexity, and dimensionality of IQ parameters which have to be assessed as well as in the method of their determining.

The German Institute for Standardization issued the national standard DIN 6868 – 161 [21] (hereinafter referred to as the DIN standard) related to acceptance testing for image quality of dental CBCT systems in 2013. As part of this introduction, completely new IQ metrics were proposed that have not been employed for quality control of clinical computed tomography (CT) x-ray equipment until now.

lence between the DIN and the IEC metrics. In addition, direct measurements of physical IQ parameters such as image contrast and noise, uniformity, and axial resolution are not supported by the new concept according to DIN.

Key points:

- ▶ The new DIN 6868 – 161 is not equivalent to the established IEC 61 223 – 3-5.
- ▶ Noise, uniformity, and contrast are well-suited to assess image artefacts.
- ▶ The implemented automated quality assurance program fits clinical routine.

Citation Format:

- ▶ Steiding C, Kolditz D, Kalender W. Comparison of Methods for Acceptance and Constancy Testing in Dental Cone-beam Computed Tomography. *Fortschr Röntgenstr* 2015; 187: 283–290

The purpose of this work was to implement two procedures for routine QA in dental CBCT, to validate the reliability of the respective IQ parameters on a clinical scanner, and to compare these results against each other. We focused on the new DIN standard and on conventional IQ metrics according to the well-established standard IEC 61 223 – 3-5 [22] in clinical CT (hereinafter referred to as the IEC standard). To allow for automated assessment of imaging performance, all IQ evaluation methods and phantom-specific detection algorithms were implemented in a dedicated computer program.

This work did not address to estimating dose in dental CBCT. Using the well-established CT dose index [6] with the standard 16 cm head phantom appears to be adequate at this point in time.

Materials and Methods

Phantoms

A new DIN-compliant phantom [21] (manufactured by QRM GmbH, Möhrendorf, Germany) is schematically depicted in **Fig. 1**. It consists of four cylindrical phantom sections, each with a diameter of 160 mm and made of polymethyl methacrylate (PMMA). A polyvinyl chloride (PVC) air test insert is embedded in the centre of phantom section 3 to determine all desired IQ parameters as stated by [21].

A modular CT IQ phantom of a previously proposed QA framework [19] (QRM GmbH, Möhrendorf, Germany) was used to measure conventional IQ metrics. Image noise, uniformity, contrast, and 3D spatial resolution were assessed [22] by using phantom sections 1–3 shown in **Fig. 2**. An optional extension ring of 160 mm in diameter and made of resin was applied to meet the spatial dimensions of the new DIN-compliant phantom.

Assessment of Imaging Performance

Image Quality Parameters According to DIN 6868 – 161

The approximated in-plane modulation transfer function (MTF), the contrast-to-noise indicator (CNI), and the uniformity indicator (UI*) were determined as stated in [21]. For this, sections 2 and 3 of the new DIN-compliant phantom were positioned in the x-ray beam in a way that all the relevant test structures were captured by the detector. In the following, the acceptance test procedure for IQ according to [21] is briefly outlined.

In-plane spatial resolution is assessed by using an approximation procedure. To calculate the approximated MTF (MTF*), the PVC-

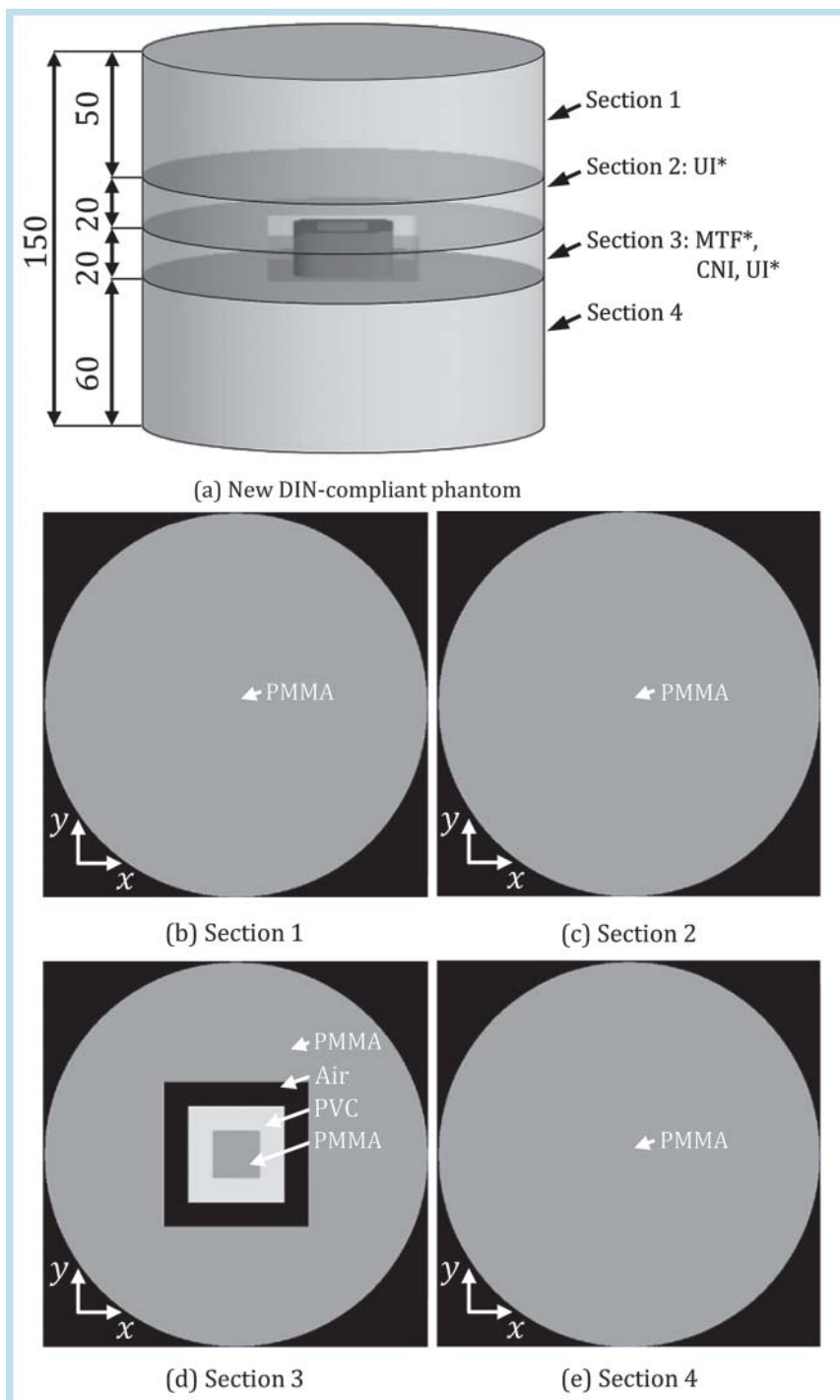


Fig. 1 Design of the new DIN-compliant phantom [21]. **a** 3-D rendered sketch of the four phantom sections (all length specifications in mm). **b–e** Ideal transverse views of sections 1–4 ($C = 0$ a. u., $W = 1000$ a. u.).

Abb. 1 Design des neuen, DIN-konformen Prüfkörpers [21]. **a** 3-D gerenderte Darstellung der vier Phantomsektionen (alle Längenangaben in mm). **b–e** Ideale, transversale Schnittbilder der Sektionen 1–4 ($C = 0$ w. E., $W = 1000$ w. E.).

air edge of phantom section 3 (• Fig. 1 d) is analysed. The post-processing of the voxels covered by a rectangular region of interest (ROI), with an edge length of 5 mm parallel to the edge and an edge length of 10 mm perpendicular to the edge, is as follows:

1. Row-by-row averaging of voxel profiles parallel to the PVC-air edge to acquire the edge spread function (ESF).
2. Computation of the line spread function (LSF) by differentiating the ESF profile.
3. Calculation of the MTF^* by averaging the moduli of the discrete Fourier-transformed LSF and the symmetrized LSF profile.

The 50% ($MTF^*_{50\%}$) and 10% MTF^* ($MTF^*_{10\%}$) values were determined from the MTF^* curve to allow for characterizing spatial resolution of the dental CBCT system.

The CNI represents the PVC-PMMA contrast in relation to the averaged noise of the PVC and PMMA compartment of phantom section 3 (• Fig. 1 d). In order to collect a representative edge profile, transverse slices of 1 mm thickness in z-direction were averaged to generate the mean image of the test insert. The pixel sequences that are in parallel to the PVC-PMMA edge are averaged row by row. Subsequently, the PVC-PMMA contrast is determined through the first and second derivative of the edge profile

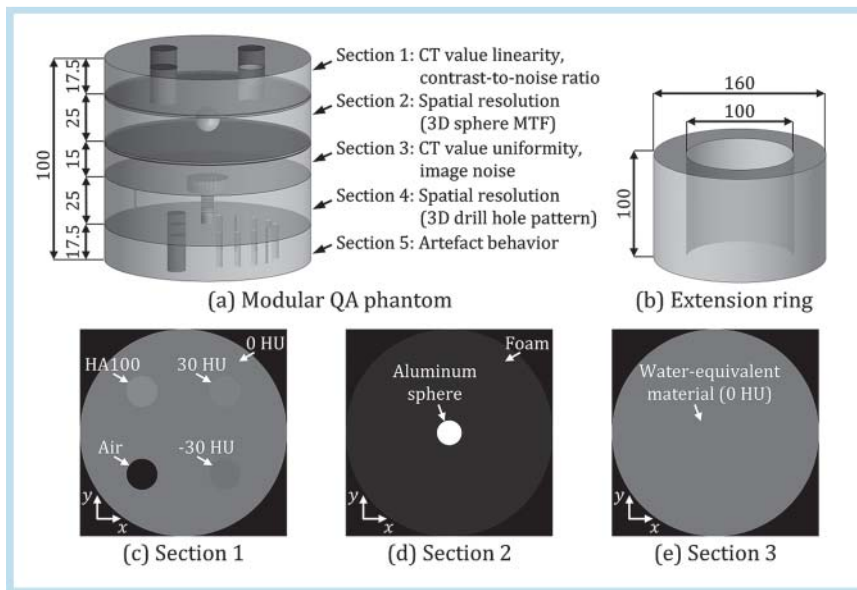


Fig. 2 Design of the modular IEC-compliant phantom [19]. 3D rendered sketch of the complete phantom consisting of five sections **a** and the optional extension ring **b**. All length specifications are in mm. **c–e** Ideal transverse views of sections 1–3 evaluated in this study ($C = 0$ a. u., $W = 1000$ a. u.).

Abb. 2 Design des modularen, IEC-konformen Prüfkörpers [19]. 3D gerenderte Darstellung des kompletten, aus fünf Sektionen bestehenden Phantoms **a** und des optionalen Erweiterungsringes **b**. Alle Längenangaben sind in mm. **c–e** Ideale, transversale Schnittbilder der in dieser Studie ausgewerteten Sektionen 1–3 ($C = 0$ w. E., $W = 1000$ w. E.).

and the noise of the PVC and PMMA compartment is estimated by the standard deviation of the respective test inserts. The UI* is defined by the PVC-PMMA contrast normalized to the most dominant non-uniformity (NU_{max}) in voxel values of phantom section 2 (► Fig. 1c). The maximum variation of the mean voxel value measured for one central (\overline{CT}_c) and four peripheral ROIs ($\overline{CT}_{p,i}$) from the average of \overline{CT}_c and $\overline{CT}_{p,i}$ (with $i = 1, \dots, 4$) corresponds to NU_{max} . We used circular ROIs, each with a diameter of 16 mm. A distance of 16 mm between the phantom border and the boundary of the peripheral ROIs was kept.

Conventional Image Quality Parameters

The conventional IQ parameters were determined in accordance with the IEC standard based on a previously proposed QA framework [19]. The volume data analysis is summarized below. More detailed information on this procedure can be found in the original paper.

Image noise and uniformity in voxel values were measured using the homogeneous phantom section 3 (► Fig. 2e). The standard deviation (σ) was computed for a circular ROI of 40 mm in diameter placed in the phantom centre to examine the amount of fluctuation in voxel values. The uniformity index (UI) [19] denotes the normalized percent difference between $\overline{CT}_{p,i}$ (with $i = 1, \dots, 4$) of the peripheral ROI labelled by i and \overline{CT}_c and allows for quantifying uniformity in voxel values. Each of these circular ROIs had a diameter of 10 mm. The peripheral ROIs were located on a circular trajectory with a radius of 35 mm and featured an angular step size of 90° .

The contrast-to-noise ratio (CNR) was determined using phantom section 1 (► Fig. 2c). We investigated the cylindrical medium-contrast insert consisting of 100 mg cm^{-3} hydroxyapatite (HA100) in relation to a water-equivalent background material. The CNR is determined as the difference in mean voxel values of a certain target and background material normalized to the standard deviation for the background material. Therefore, two cylindrical volumes of interest (VOIs), each with a diameter of 9 mm and a height of 7.5 mm, were positioned on the inner part of the inserts.

Comprehensive evaluation of volumetric spatial resolution is still an above-standard procedure for quality control of clinical CT x-

Table 1 List of abbreviations.

Tab. 1 Abkürzungsverzeichnis.

3 D	three-dimensional
a. u.	arbitrary units
CBCT	cone-beam computed tomography
cm	centimetre
CNI	contrast-to-noise indicator
CNR	contrast-to-noise ratio
CT	computed tomography
DIN	German Institute for Standardization
FOM	field of measurement
HA100	100 mg cm^{-3} hydroxyapatite
IEC	International Electrotechnical Commission
kV	kilovoltage
mAs	milliamperere-second
mm	millimetre
MTF	modulation transfer function
MTF*	approximated MTF
PMMA	polymethyl methacrylate
PVC	polyvinyl chloride
UI	uniformity index
UI*	uniformity indicator

ray equipment, but it is conform to [22] by all means. 3D MTFs were calculated from measurements of the spherical edge of phantom section 2 (► Fig. 2d). The ESFs corresponding to the step response in the x -, y -, and z -direction as well as in the xy -plane were sampled by a trilinear interpolation as a function of radial distance from the centre of the sphere. The ESF profiles were differentiated with respect to the radial distance to obtain the corresponding LSF. The exact MTF was computed by taking the modulus of the discrete Fourier-transformed LSF. This technique was performed for all direction-specific components of the 3D spatial resolution. As figures of merit, the 50% ($MTF_{50\%}$) and 10% MTF ($MTF_{10\%}$) values were tracked for each type of the MTFs.

Automated Volume Data Analysis

To correctly assess all desired IQ parameters and, in consequence, to achieve high reliability of the measured imaging performance, the ROIs and VOIs must be accurately centred and aligned in the reconstructed volume data set. For this purpose, we developed automated detection algorithms for both types of QA phantoms described in section 2.1, which were integrated in a dedicated computer program (ImpactIQ, CT Imaging GmbH, Erlangen, Germany). The registration processes are based solely on the CT volumes without the need of external markers or strict phantom alignment to allow for easy-to-use quality control in clinical routine.

The detection algorithm for the new DIN-compliant phantom was implemented in C++ employing a multi-step approach as follows:

1. Initialization of the evaluation program including read-in of the reconstructed volume data set.
2. Calculation of the z-vector of the phantom.
3. Calculation of the spatial shift of the phantom.
4. Calculation of the x- and y-vector of the phantom.

The phantom segmentation was performed analogous to [19]

The detection of the IEC-compliant phantom was realized applying the procedure described in [19].

Both detection algorithms provide the position off-centre and the orientation of the phantoms. As a result of this, the groups of ROIs and VOIs needed for evaluating all IQ aspects are arranged according to the strategies specified in section 2.2.

Setup for Measurements

Measurements were performed on a dental CBCT system (KaVo 3 D eXam, KaVo Dental GmbH, Biberach/Riß, Germany) installed at the University Medical Centre of Erlangen, Germany. The data acquisition and reconstruction parameters used correspond to a predefined standard clinical protocol and are listed in **Table 2**. The reconstructed volume data sets were exported as uncompressed DICOM images provided by the dental CBCT system.

Both QA phantoms were centred at two different axial distances from the centre of the field of measurement (FOM) ($z = 0$ cm and $z = 6$ cm). This makes an evaluation of the effect of the phantom location and, in consequence, the severity of image artefacts feasible.

Results

The position and orientation of the phantoms were detected fully automatically in all these measurements. Thus, a reproducible placement of the evaluation regions and volumes was provided. This was initially verified by visual inspection of the ROIs and VOIs marked in the volume data sets.

The IQ parameters determined in this study are summarized in **Table 3**. Representative transverse views of the phantom sections used for assessment of imaging performance in dental CBCT according to the standards [21] and [22] are depicted in **Fig. 3, 4**. The reconstructed images correspond to two different axial positions and have an identical display window level.

The difference in measuring at $z = 0$ cm and $z = 6$ cm was most prominently observed for the homogeneous phantom sections. This was also confirmed quantitatively by the determined IQ parameters listed in **Table 3**. With increasing axial distance from the centre of the FOM, UI* and CNI fell by 30% and 19%, respectively. Conventional IQ parameters by means of the UI

Table 2 Scan and reconstruction parameters for the measurements carried out on the dental CBCT system KaVo 3 D eXam.

Tab. 2 Aufnahme- und Rekonstruktionsparameter für die Experimente, welche an dem DVT-Gerät KaVo 3 D eXam ausgeführt wurden.

parameters	settings
scan protocol	standard
scan trajectory	circular
tube voltage / kV	120
tube current-exposure time product / mAs	18.54
field of measurement / cm ³	16 × 16 × 13
reconstruction kernel	– (default)
reconstructed volume / voxel	536 × 536 × 440
reconstructed voxel size / mm ³	0.3 × 0.3 × 0.3

Table 3 Image quality parameters according to [21] (new) and IEC-compliant procedures (conv.) measured at two different axial positions. For comparative purposes, the percent difference of the results at the peripheral FOM ($z = 6$ cm) to the centre ($z = 0$ cm) is also listed.

Tab. 3 Bildqualitätsparameter gemäß [21] (new) und IEC-konformen Prozeduren (conv.), welche an zwei unterschiedlichen, axialen Positionen gemessen wurden. Der prozentuale Unterschied zwischen den Ergebnissen für das periphere Messfeld ($z = 6$ cm) und dem Messfeldzentrum ($z = 0$ cm) wird für vergleichende Zwecke ebenfalls aufgeführt.

IQ parameters	z = 0 cm	z = 6 cm	difference / %
<i>uniformity</i>			
UI* (new)	27.42	19.19	–30.0
UI (conv.) / %	4.09	–3.98	–197.3
<i>image contrast</i>			
CNI (new)	26.96	21.84	–19.0
CNR (conv.)	3.97	2.52	–36.5
<i>resolution</i>			
MTF _{50%} ⁺ (new) / cm ^{–1}	4.78	4.70	–1.7
MTF _{10%} ⁺ (new) / cm ^{–1}	8.20	8.15	–0.6
MTF _{50%,xy} ⁺ (conv.) / cm ^{–1}	4.75	4.65	–2.1
MTF _{10%,xy} ⁺ (conv.) / cm ^{–1}	8.57	8.41	–1.9
MTF _{50%,z} ⁺ (conv.) / cm ^{–1}	4.75	4.18	–12.0
MTF _{10%,z} ⁺ (conv.) / cm ^{–1}	9.04	8.97	–0.8
<i>image noise</i>			
σ(conv.) / a. u.	33.01	38.83	17.6

and the CNR provided sensitivity to the dependence of the phantom position by a factor of about 2 to 7 times higher than for the new DIN standard; i.e., UI and CNR were reduced by 197.3% and 36.5%, respectively. Image noise was increased by about 18%. Moreover, the identification of cupping and capping artefacts in the reconstructed volume data sets was feasible with the UI indicated by a positive and negative value, respectively. Good consistency between this quantitative uniformity analysis and the visual perception of the associated transverse slices shown in **Fig. 4c, f** was achieved.

For the assessment of high-contrast spatial resolution, the MTFs of the dental CBCT system using the approximated as well as the exact calculation procedure are presented in **Fig. 5**. The resulting curves were well comparable in shape. As shown in **Table 3**, 50% and 10% in-plane MTF values from the approximated and the exact MTF methodology were in agreement to within 5%. Furthermore, no significant difference between both measurements at $z = 0$ cm and measurements at $z = 6$ cm

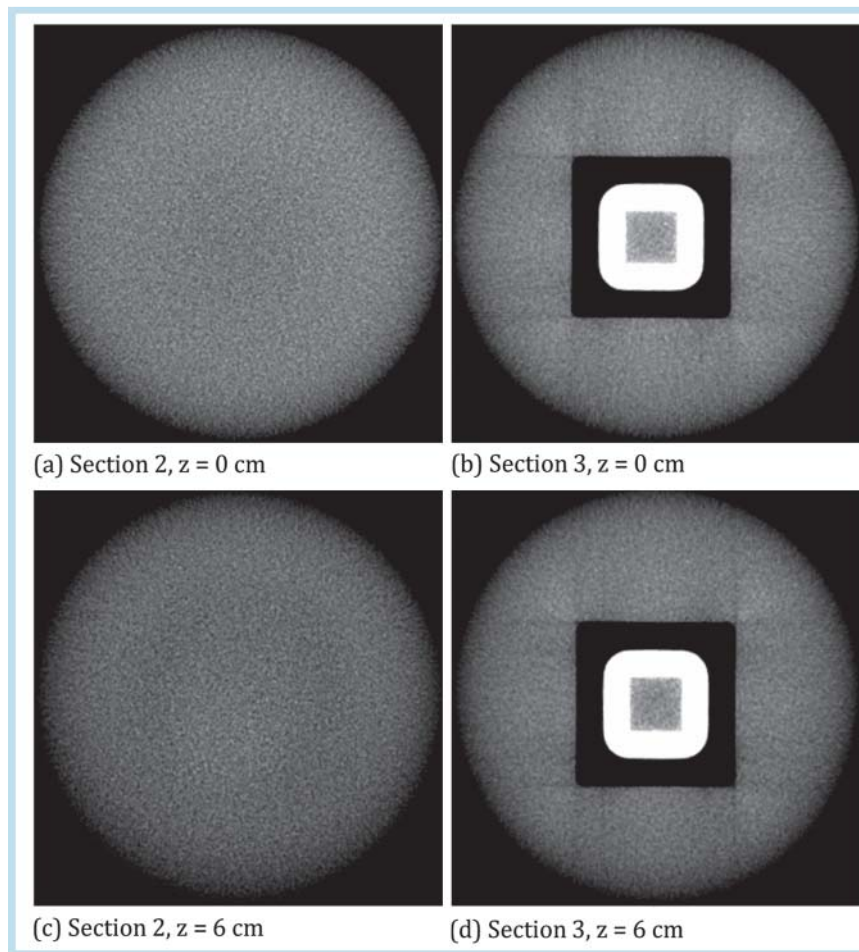


Fig. 3 Transverse views of the sections 2 and 3 of the new DIN-compliant phantom [21] centred at two different axial positions ($z = 0$ cm and $z = 6$ cm). The images are windowed identically ($C = 0$ a. u., $W = 800$ a. u.).

Abb. 3 Transversale Schnittbilder von den Sektionen 2 und 3 des neuen, DIN-konformen Prüfkörpers [21], welcher an zwei unterschiedlichen, axialen Positionen ($z = 0$ cm und $z = 6$ cm) zentriert wurde. Die Bilder besitzen eine identische Fensterung ($C = 0$ w. E., $W = 800$ w. E.).

was observed for in-plane resolution regardless of the calculation procedure. By comparing the in-plane 50% and 10% MTF values with those in z -direction, the dental CBCT system showed almost isotropic 3D high-contrast spatial resolution.

Discussion

As for all new tomographic imaging devices, the compliance of physical imaging characteristics with specifications needs to be verified in clinical practice. However, presently, there are competing methodologies for acceptance and constancy testing for image quality in CT.

The DIN standard represents an important step for quality control in dental CBCT since it denotes the first national consensus on acceptance testing for IQ of this modality. This standard focuses on a broad range of dedicated CBCT scanners differing in their architecture, technical equipment, and output data format. However, the introduction of completely new IQ metrics might be brought into question since the functional principle of the dental CBCT devices is quite comparable to conventional CT systems and the manufacturers claim full 3D capability. Furthermore, a direct interpretation of physical imaging characteristics through the new metrics UI^* and CNI is not possible. In other words, correct analysis of both uniformity and image contrast is not provided by the new methodology according to the in-

structions stated in section 4.3.7 and appendix B of [21] insofar the former is defined by differences in mean voxel values measured in the centre and periphery and the latter is defined by the mean voxel value of a certain target material after subtraction of the mean voxel value of the background material. The optional assessment of well-established IQ parameters as an amendment to the existing acceptance testing standard for IQ in dental CBCT is desirable. A proof of concept for determining image noise, CT value accuracy and uniformity, contrast, and 3D resolution has already been successfully performed in previous studies on different dental CBCT systems of various manufacturers considering several acquisition volumes [17–19, 23, 24]. This may also contribute to refine the upcoming constancy testing standard 6868–15 for IQ in dental CBCT.

According to the recently updated German quality assurance guideline [25], the new DIN 6868–161 shall only be applied when a corresponding constancy testing standard 6868–15 is finalized. Until then, acceptance testing for IQ in dental CBCT has to be performed according to the procedures described in [25]. However, this guideline and the DIN standard differ in IQ parameters which have to be assessed; e. g. image noise and CT value accuracy are addressed by [25] but not by DIN. In consequence, acceptance and constancy testing procedures still need to be harmonized.

Our study confirmed that evaluating phantom sections 1, 2, and 3 of the modular IEC-compliant phantom appears to be sufficient to assess imaging performance for quality control purposes in

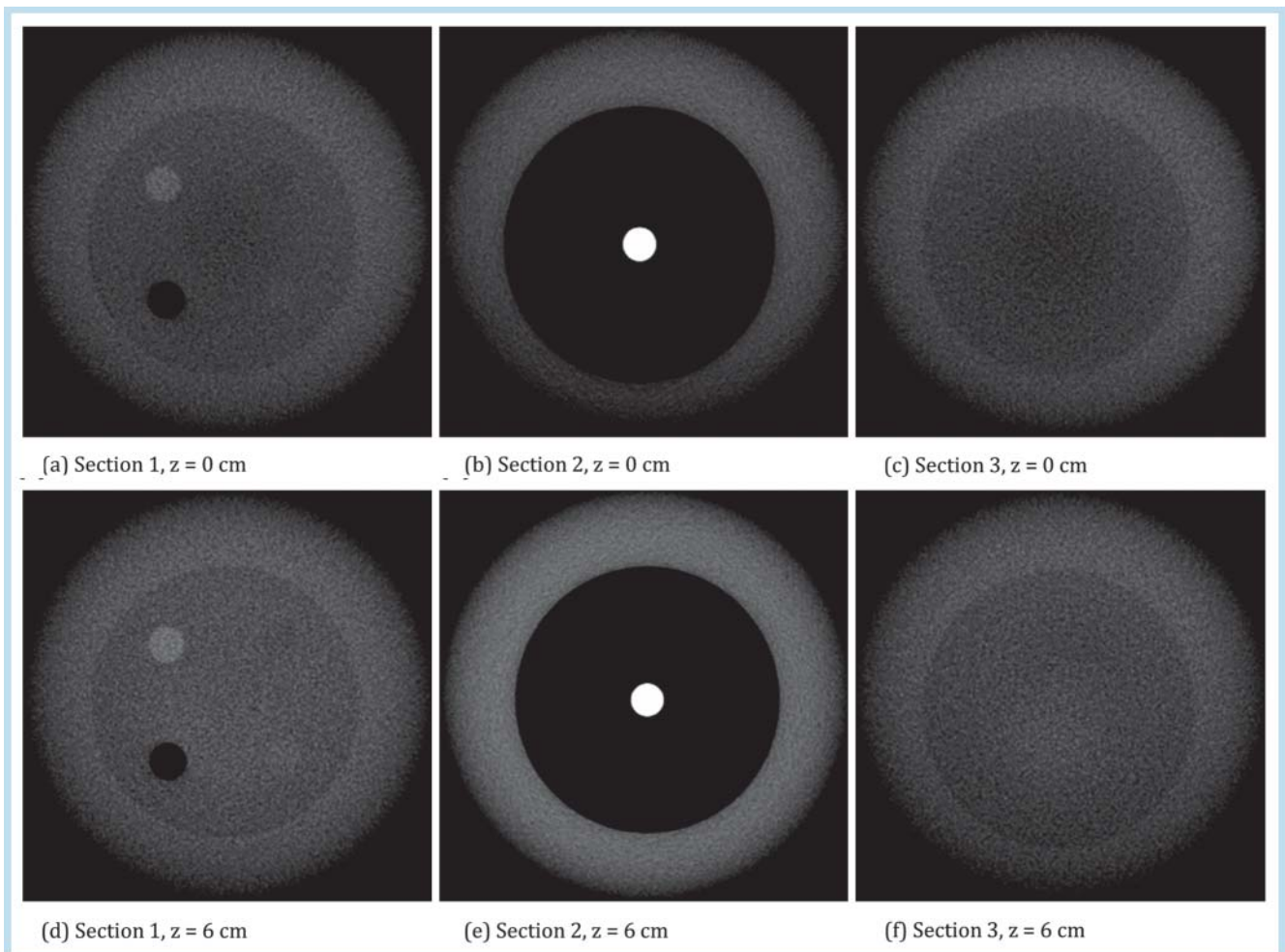


Fig. 4 Transverse views of the sections 1–3 of the modular IEC-compliant phantom [19] centred at two different axial positions ($z = 0$ cm and $z = 6$ cm). The images are windowed identically ($C = 0$ a. u., $W = 800$ a. u.).

Abb. 4 Transversale Schnittbilder von den Sektionen 1–3 des modularen, IEC-konformen Prüfkörpers [19], welcher an zwei unterschiedlichen, axialen Positionen ($z = 0$ cm und $z = 6$ cm) zentriert wurde. Die Bilder besitzen eine identische Fensterung ($C = 0$ w. E., $W = 800$ w. E.).

clinical CT objectively. This configuration of the modules allows for the measurement of image noise, uniformity, contrast, and 3D resolution. Thus, the conformity to the IEC standard is met and the equivalence to the new DIN standard is considered to be ensured.

Our measurements revealed that the position of the QA phantoms plays an important role for image quality control in CBCT. The conventional IQ parameters were more sensitive to image artefacts. So, determining the standard deviation, the UI, and the CNR appears to be well-suited to identify possible degradations of the apparatus at an early stage, as indicated in [Table 3](#).

Evaluating only planar IQ parameters in the isocentre of the scanner turned out to be inadequate for the comprehensive characterisation of imaging performance in CBCT, as confirmed by the results in [Table 3](#). Physical IQ aspects with respect to image noise, uniformity, contrast, and resolution depend critically on their direction and position [19]. Consequently, the assessment of essential objective IQ metrics, e.g. standard deviation, UI, CNR, and 3D MTF in the complete FOM, are considered to be necessary after a new device has been installed or major modifications have been made to existing equipment.

In conclusion, there is no similarity between the recently proposed metrics [21] and the well-established CT IQ assessment [22]. In addition, direct measurements of physical image characteristics such as image noise, uniformity, contrast, and axial resolution are not supported by the new concept according to DIN 6868–161.

Clinical Relevance of the Study

- ▶ Acceptance and constancy testing are a necessity for clinical computed tomography (CT) systems and need to be harmonized and established for cone-beam CT (CBCT).
- ▶ Distinct differences between the new DIN 6868–161 and the established IEC 61 223–3-5 have been recognized and should be taken into account for the upcoming standard DIN 6868–15 for constancy testing in dental CBCT.

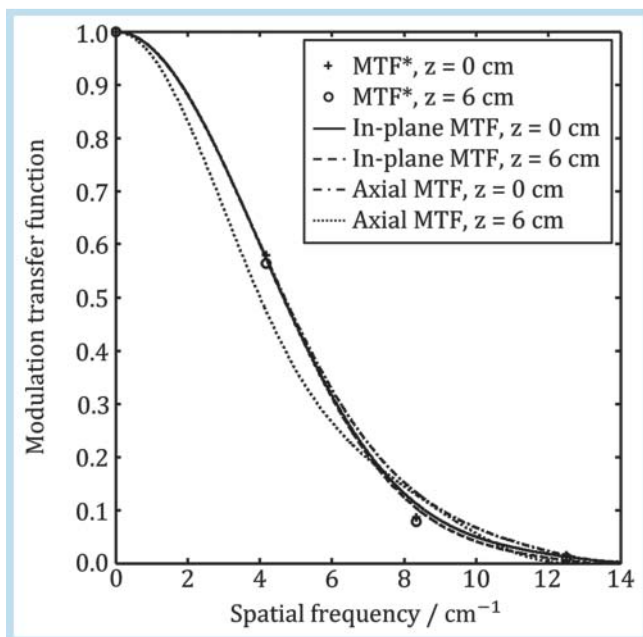


Fig. 5 Representative MTFs of the dental CBCT system measured at the two axial positions $z = 0$ cm and $z = 6$ cm.

Abb. 5 Repräsentative MÜFs des DVT-Gerätes, welche an den beiden axialen Positionen $z = 0$ cm und $z = 6$ cm gemessen wurden.

Acknowledgements

The authors wish to thank Friedrich W. Neukam, University Medical Centre of Erlangen Germany, who provided access to the clinical dental CBCT system. The present work was performed in partial fulfillment of the requirements for obtaining the degree “Dr. rer. biol. hum.” at the Friedrich-Alexander-University Erlangen-Nürnberg of the first author.

References

- 1 Mozzo P, Procacci C, Tacconi A et al. A new volumetric CT machine for dental imaging based on the cone-beam technique: preliminary results. *Eur Radiol* 1998; 8: 1558–1564
- 2 Arai Y, Tammisalo E, Iwai K et al. Development of a compact computed tomographic apparatus for dental use. *Dentomaxillofac Radiol* 1999; 28: 245–248
- 3 Vannier MW. Craniofacial computed tomography scanning: technology, applications and future trends. *Orthod Craniofac Res* 2003; 6: 23–30
- 4 Holberg C, Steinhäuser S, Geis P et al. Cone-beam computed tomography in orthodontics: benefits and limitations. *J Orofac Orthop* 2005; 66: 434–444
- 5 Hatcher DC. Operational principles for cone-beam computed tomography. *J Am Dent Assoc* 2010; 141: 3S–6S
- 6 Kalender WA. *Computed Tomography: Fundamentals, System Technology, Image Quality, Applications*. 3rd ed. Erlangen: Publicis Publishing; 2011

- 7 Suomalainen A, Kiljunen T, Käser Y et al. Dosimetry and image quality of four dental cone beam computed tomography scanners compared with multislice computed tomography scanners. *Dentomaxillofac Radiol* 2009; 38: 367–378
- 8 Ludlow JB, Ivanovic M. Comparative dosimetry of dental CBCT devices and 64-slice CT for oral and maxillofacial radiology. *Oral Surg Oral Med Oral Pathol Oral Radiol Endod* 2008; 106: 106–114
- 9 Eggers G, Klein J, Welzel T et al. Geometric accuracy of digital volume tomography and conventional computed tomography. *Br J Oral Maxillofac Surg* 2008; 46: 639–644
- 10 Dalchow CV, Weber AL, Yanagihara N et al. Digital volume tomography: radiologic examinations of the temporal bone. *Am J Roentgenol* 2006; 186: 416–423
- 11 Hatcher DC, Aboudara CL. Diagnosis goes digital. *Am J Orthod Dentofacial Orthop* 2004; 125: 512–515
- 12 Heiland M, Schulze D, Rother U et al. Postoperative imaging of zygomaticomaxillary complex fractures using digital volume tomography. *J Oral Maxillofac Surg* 2004; 62: 1387–1391
- 13 Schulze R, Hassfeld S, Schulze D et al. S1-Empfehlung: Dentale Volumentomographie (DVT). *Dtsch Zahnärztl Z* 2009; 64: 490–496
- 14 Health Protection Agency. Recommendations for the design of X-ray facilities and quality assurance of dental Cone Beam CT (Computed Tomography) systems HPA-RPD-065. Chilton: Health Protection Agency; 2010
- 15 Carter L, Farman AG, Geist J et al. American Academy of Oral and Maxillofacial Radiology executive opinion statement on performing and interpreting diagnostic cone beam computed tomography. *Oral Surg Oral Med Oral Pathol Oral Radiol Endod* 2008; 106: 561–562
- 16 Horner K, Islam M, Flygare L et al. Basic principles for use of dental cone beam computed tomography: consensus guidelines of the European Academy of Dental and Maxillofacial Radiology. *Dentomaxillofac Radiol* 2009; 38: 187–195
- 17 Vassileva J, Stoyanov D. Quality control and patient dosimetry in dental cone beam CT. *Radiat Prot Dosimetry* 2010; 139: 310–312
- 18 Pauwels R, Stamatakis H, Manousaridis G et al. Development and applicability of a quality control phantom for dental cone-beam CT. *J Appl Clin Med Phys* 2011; 12: 245–260
- 19 Steiding C, Kolditz D, Kalender WA. A quality assurance framework for the fully automated and objective evaluation of image quality in cone-beam computed tomography. *Med Phys* 2014; 41: 031901
- 20 SEDENTEXCT Guideline Development Panel. Radiation Protection: Cone Beam CT for Dental and Maxillofacial Radiology. Evidence based guidelines. A report prepared by the SEDENTEXCT project; 2011, Available on: www.sedentext.eu
- 21 Deutsches Institut für Normung (DIN). “Sicherung der Bildqualität in röntgendiagnostischen Betrieben – Teil 161: Abnahmeprüfung nach RöV an zahnmedizinischen Röntgeneinrichtungen zur digitalen Volumentomographie,” DIN Report Nr. 6868-161 (DIN, Berlin, 2013)
- 22 International Electrotechnical Commission (IEC). “Evaluation and routine testing in medical imaging departments – Part 3–5: Acceptance tests – Imaging performance of computed tomography X-ray equipment,” IEC Report No. 61223-3-5. Geneva: IEC; 2004
- 23 Kyriakou Y, Kolditz D, Langner O et al. Digital volume tomography (DVT) and multislice spiral CT (MSCT): an objective examination of dose and image quality. *Fortschr Röntgenstr* 2011; 183: 144–153
- 24 Blendl C, Fiebich M, Voigt JM et al. Investigation on the 3 D geometric accuracy and on the image quality (MTF, SNR and NPS) of volume tomography units (CT, CBCT and DVT). *Fortschr Röntgenstr* 2012; 184: 24–31
- 25 Bundesministerium für Umwelt, Naturschutz, Bau und Reaktorsicherheit (BMU). “Richtlinie zur Durchführung der Qualitätssicherung bei Röntgeneinrichtungen zur Untersuchung oder Behandlung von Menschen nach den §§ 16 und 17 der Röntgenverordnung – Qualitätssicherungs-Richtlinie (QS-RL),” Berlin: BMU; 2014